Fachtagung "Experimentelle Strömungsmechanik"
5. – 7. September 2017, Karlsruhe

Eindimensional expliziter Druck explizite Sättigung (EPES) Model für Methanhydrat Dissoziation durch Druckentlastung

One-dimensional explicit pressure explicit saturation (EPES) model for methane hydrate dissociation by depressurization

G. Luzi[1], T. Kim[1], J. R. Agudo[1], R. Saur[1], S. Loekman[2], C. Rauh[1,3,4], A. Delgado[1,4]

[1]Institute of Fluid Mechanics, FAU Busan Campus, University of Erlangen-Nuremberg,
46-742 Busan, Republic of Korea
[2]Institute of Chemical Reaction Engineering, FAU Busan Campus, University of Erlangen-Nuremberg,
46-742 Busan, Republic of Korea
[3]Department of Food Biotechnology and Food Process Engineering
Technische Universität Berlin, D-14195 Berlin, Germany
[4]Institute of Fluid Mechanics, University of Erlangen-Nuremberg,
D-91058 Erlangen, Germany

Gashydrat (GH), Dissoziation, Druckentlastung, Nummerische Simulation
Gas hydrates (GHs), Dissociation, Depressurization, Numerical simulations

Abstract

One of the most attractive characteristics of gas hydrates (GHs) is that they contain a high amount of natural gas per unit volume. Natural gas is produced on large-scales by different processes that can be grouped into three categories: depressurization, thermal stimulation and inhibitor injection. Depressurization of a reservoir is usually done by drilling a well into it, in order to reduce the pressure and bring the hydrate outside of the thermodynamic stability conditions. When this happens, dissociation starts, thus water and gas form. To date, the transport phenomena involved during depressurization are not well understood yet.
In this study, we numerically model the dissociation of methane hydrate in a porous sandstone core due to depressurization. For simplicity, we consider a one-dimensional geometry, and we solve the highly nonlinear strongly coupled set of governing equations of saturations, pressure and temperature by means of an explicit fifth order Runge-Kutta-Fehlberg method, retaining a second order discretization in space. Our numerical results recover qualitatively well the trend of experimental data found in literature, and our numerical scheme is easier to implement with respect to implicit formulations.

Introduction

Natural gas hydrates (GHs) are crystalline solid composed of water and gas, resembling packed snow or ice. Gas molecules are encaged inside a crystal structure composed of water molecules (Sloan and Koh, 2008). It is estimated that 1 m^3 of hydrate dissociating at atmospheric pressure forms 164 m^3 of natural gas and 0.8 m^3 of water (Kvenvolden, 1993). Besides, the estimated amount of natural gas trapped in gas hydrates is much greater than that available in the conventional known reserves. Therefore, GHs have also the potential to be an interesting alternative source of natural gas.

In order to produce natural gas, GHs need to be dissociated first. The conventional ways for dissociating hydrate consist of increasing temperature, adding inhibitors and decreasing pressure. In all the three cases, hydrate is brought outside of the stability region and it dissociates. Fluctuations in pressure, temperature, salinity, degree of gas saturation or sediment bed properties may cause hydrate to dissociate. Several laboratory scale experiments and simulations have been embarked to investigate the hydrate dissociation in a sandstone core of standard dimensions. A one dimensional model, able to simulate the dissociation process of methane hydrate (MH) has been developed (Sun et al., 2005). They investigate the influence of the surrounding and longitudinal heat transfer coefficient and conclude that the surrounding heat transfer coefficient strongly influences the gas production, while the well temperature does not affect the gas production significantly. Moreover, they are able to distinguish two dissociation regimes, one is flow controlled and the other one is dissociation controlled. Using a two-dimensional axisymmetric model, numerical studies have shown how different boundary and initial conditions, i.e. different outlet pressure and initial temperature values, affect the water phase during MH dissociation process (Zhao et al., 2012). At the beginning of the process, a higher amount of water slows down the pressure decrease inside the core and afterwards heat transfer effects prevail. Even though thermal conductivity of water is higher than that of gas, the convection heat transfer due to gas is greater than that of water, since gas moves much faster than water. Different depressurization methods have also been investigated using also a two dimensional axisymmetric model (Xuke et al., 2012). Variations of the initial pressure difference between the core and the surrounding affect the final gas production, while changes in the pressure rate affect the hydrate dissociation time. On the one hand, the larger the depressurization range, the higher the gas accumulation is but on the other hand, a faster depressurization reduces the hydrate dissociation time. Additionally, the sediment thermal conductivity does not significantly affect the gas production, but higher surrounding temperatures increase both gas accumulation and production rate. A two-dimensional simulator to investigate both hydrate formation and dissociation has been developed (Sun and Mohanty, 2006). It is able to handle five phases, i.e. water, gas, hydrate, ice and salt precipitates. On the one hand, increasing initial temperature, decreasing the outlet pressure, introducing salts, and increasing boundary heat transfer coefficient accelerates the hydrate dissociation process. On the other hand, higher outlet temperatures with lower global boundary heat coefficients decelerate the process.

In this work, we present a one-dimensional model for the simulation of MH dissociation by depressurization in a sandstone core. We discretize the governing equations of pressure, saturations and temperature by second order accurate finite difference methods, and we integrate them with a fifth order explicit method. Afterwards, we compare our numerical results to the experiments performed by (Masuda et al., 1999). Our numerical results matched the experimental data in terms of trend and the amount of gas produced over the time. It is also worth mention that our numerical results do not show any strong pressure or temperature delay with time among different sections of the core as reported by other models (Nazridoust and Ahmadi, 2007) (Zhao et al., 2012).

Theoretical part

The mass balance equations for gas, water and hydrate can be written as

$$\frac{\partial}{\partial t}(\phi \rho_g S_g) = -\frac{\partial}{\partial x}\left(\rho_g v_{gx}\right) + \dot{m}_g \qquad 1$$

$$\frac{\partial}{\partial t}(\phi\rho_w S_w) = -\frac{\partial}{\partial x}(\rho_w v_{wx}) + \dot{m}_w \quad (2)$$

$$\frac{\partial}{\partial t}(\phi\rho_h S_h) = -\dot{m}_h \quad (3)$$

where S_g , S_w and S_h indicate gas, water and hydrate saturation respectively. ϕ is the porosity of the core and ρ_g , ρ_w and ρ_h are the density of gas, water and hydrate respectively. t denotes time and x is the coordinate of the axial direction. v_{gx} and v_{wx} are the velocity of the gas and water phase along the x direction, respectively. $\dot{m}_g$ and $\dot{m}_w$ are the gas and water generation rates, while $\dot{m}_h$ is the hydrate dissociation rate. They are modelled according to the equations of (Kim et al., 1987). Saturation is defined as the ratio between the volume occupied by a medium in a void of a porous material and the whole volume of the void. It is defined as

$$S_i = \frac{V_i}{V_{void}} \quad (4)$$

where V denotes volume and $i = g, w, h$.

The velocities of both gas and water phases are expressed through the Darcy law (Nazridoust and Ahmadi, 2007)

$$v_{gx} = -\frac{KK_{rg}}{\mu_g}\frac{\partial p_g}{\partial x} \quad (5)$$

$$v_{wx} = -\frac{KK_{rw}}{\mu_w}\frac{\partial p_w}{\partial x} \quad (6)$$

where p_g and p_w are the pressure of gas and water, μ_g and μ_w are the viscosities of gas and water. K is the absolute permeability, which is function of the hydrate saturation S_h (Masuda et al., 1999)

$$K = K_0(1 - S_h)^n \quad (7)$$

where K_0 is the intrinsic permeability and n is permeability reduction index, which depends on the structure of the porous medium, and it is determined experimentally (Nazridoust and Ahmadi, 2007). Here, we use the values of $K_0 = 9.798 \cdot 10^{-10}$ cm^{-2} and $n = 10$. For the relative permeability of both gas and water, we implement the Corey model (Brooks and Corey, 1964). By adding Eqs. (1-3), expressing the velocity components with Eq. (5-6) and taking into account the relationship

$$S_h + S_w + S_g = 1 \quad (8)$$

we obtain an equation for the pressure of the gas

Karlsruhe, Germany, ISBN 978-3-9816764-3-3

$$\frac{\partial p_g}{\partial t} = \frac{1}{\frac{\partial \rho_g}{\partial P_g}} \frac{1}{\phi S_g} \left[\frac{\partial}{\partial x} \left(\rho_g \frac{K k_{rg}}{\mu_g} \frac{\partial p_g}{\partial x} \right) + \dot{m}_g \right] + \frac{1}{\frac{\partial \rho_g}{\partial P_g}} \frac{\rho_g}{\phi S_g \rho_w} \left[\frac{\partial}{\partial x} \left(\rho_w \frac{K k_{rw}}{\mu_w} \frac{\partial \left(p_g - p_c \right)}{\partial x} \right) + \dot{m}_w \right] + \frac{1}{\frac{\partial \rho_g}{\partial P_g}} \frac{\rho_g}{\phi S_g \rho_h} \dot{m}_h \tag{9}$$

The pressures of both fluids are related via the capillary pressure, i.e.

$$p_c = p_g - p_w \tag{10}$$

where p_c is formulated as a function of water and gas saturation in the Corey model (Brooks and Corey, 1964). It is expressed as

$$p_c = p_c^e \left(\frac{\frac{S_w}{S_w + S_g} - S_{wr}}{1 - S_{wr}} \right)^{-n_c} \tag{11}$$

Here, p_c^e is the entry pressure and n_c is the pore size distribution coefficient. In our case $p_c^e = 10^{-3}$ MPa, $n_c = 0.65$, and $S_{wr} = 0.2$. S_{wr} is the residual water saturation.
The energy equation reads

$$\frac{\partial}{\partial t} \left[\phi \left(\rho_g S_g h_g + \rho_w S_w h_w + \rho_h S_h h_h \right) + \left(1 - \phi \right) \rho_s h_s \right] = + \frac{\partial}{\partial x} \left(\lambda_c \frac{\partial T}{\partial x} \right) - \frac{\partial}{\partial x} \left(\rho_g v_{gx} h_g + \rho_w v_{wx} h_w \right) + q \tag{12}$$

where T is the temperature, h_h, h_g and h_w are the enthalpies of hydrate, gas and water, respectively. The effective thermal conductivity coefficient reads

$$\lambda = \lambda_s \left(1 - \phi \right) + \phi \left(\lambda_h S_h + \lambda_g S_g + \lambda_w h_w \right) \tag{13}$$

where λ_s, λ_h, λ_g and λ_w are the thermal conductivity coefficients of sediment, hydrate, gas and water, respectively. From the ideal gas law, the density of gas is related to the temperature T and the pressure p_g via the relation

$$\frac{p_g}{\rho_g} = \frac{RT}{M_g} \tag{14}$$

where R is the universal gas constant and M_g is the molecular weight of gas. Finally, the heat transfer from the surrounding environment q is defined as (Sun et al., 2005)

$$q = \frac{A_L}{V} \alpha \left(T_s - T \right) \tag{15}$$

Karlsruhe, Germany, ISBN 978-3-9816764-3-3

where V is the volume and A_L is the lateral surface of the cylindrical core. α is the heat transfer coefficient and T_s is the surrounding temperature.

Problem setup

We cover the domain with a one-dimensional grid with 40 points equally spaced along the x direction. We define a pressure outlet at the location $x = 0$ and an adiabatic boundary condition at $x = L$. In formulas, the initial conditions are as follows

$t = 0$ s

$$p_0 = 3.75 \text{ MPa and } T_0 = 275.15 \text{ K } \quad 0 \le x \le L \tag{16}$$

$$S_{w0} = 0.207 \quad S_{g0} = 0.35 \quad S_{h0} = 0.443 \quad 0 \le x \le L$$

while the boundary conditions read

$t > 0$ s

$$p = 2.84 \text{ MPa and } p_c = p_c^e \text{ at } x = 0 \tag{17}$$

$$\frac{\partial p}{\partial x} = 0 \text{ and } \frac{\partial T}{\partial x} = 0 \text{ at } x = 0 \text{ at } x = L$$

Additionally, we define a free convective heat transfer between the core and the surrounding, which is included in Eq. (12). We discretize the system of Eqs. (1-3), (9) and (12), by means of a second order central difference scheme in space, and we integrate them in time by means of a robust fifth order Runge-Kutta Fehlberg method. The time step $\Delta t = 1.56 \cdot 10^{-4}$ s is held constant. Additionally, we discretize the boundary conditions Eq. (21) with a third order polynomial curve.

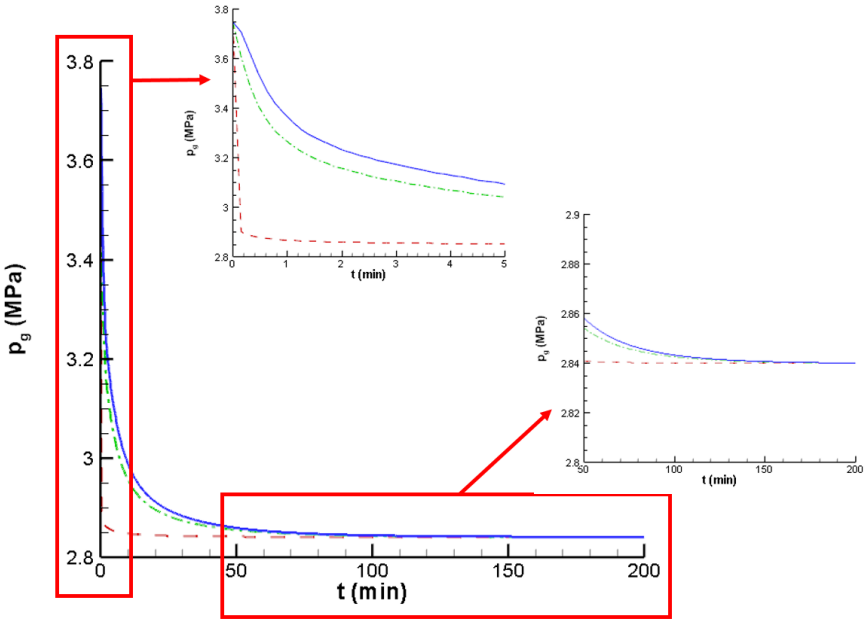

Figure 1 Pressure change with time at three different sections of the sandstone core. Red dashed line at x=0.75 cm, green dashed dot line at x=15 cm, and blue solid line at x=22.5 cm. The two insets depict a zoom of the pressure decay at three different sections of the sandstone core. Red dashed line at x=0.75 cm, green dashed dot line at x=15 cm and blue solid line at x=22.5 cm. top) first five minutes of the process and right) the last 150 minutes

Karlsruhe, Germany, ISBN 978-3-9816764-3-3

Results and discussion

After the dissociation starts, the gas pressure at different sections of the core quickly decreases with time, see Figure 1. The gas pressure at the section $x = 0.75$ cm, close to the inlet, strongly drops after approximately ten seconds, reaching almost the final value, see the zoom on top of Figure 1. At the other two sections, i.e. at $x = 15$ cm and at $x = 22.5$ cm the pressure drops considerably after approximately ten minutes. Afterwards, the pressure slowly decreases until it completely reaches the final value after about 150 minutes, see the zoom on the right of Figure 1. At the beginning of the process, the pressure difference between the core and the surrounding pushed gas and water out of the sandstone core. As both fluids leave the core, the pressure difference between the core and the surroundings decreases. Therefore, the force that drives the fluids out of the core decreases. Besides, the low values of porosity and permeability further slows down the pressure decrease and therefore the dissociation process.

The competition between the endothermic reaction and heat flow from the surroundings determines the temperature of the phases inside the core. Initially, since the temperature of the core equals the surroundings one, it decreases due to the endothermic reaction, reaching a minimum after about twenty minutes, see Figure 2. Afterwards, due to the temperature difference between the surroundings and the core, the heat transfer energy due to conduction and convection exceeds the heat sink due to the endothermic reaction, and the temperature increases until it reaches the initial value. The front part of the core reaches the minimum faster, at slightly lower values. The reason is the higher heat consumption by hydrate dissociation, due to the faster decrease of the pressure. The lower minimum temperature reached results also in a faster temperature increase.

The cumulative methane gas computed numerically was compared with the values measured experimentally (Masuda et al., 1999), as can be seen in Figure 3. Numerical predictions are qualitatively in good accordance with experimental results, and the monotonically increase trend of gas generation is recovered. The total amount of generated gas predicted by the numerical simulations after approximately 200 minutes is 8587.25 cm^3, which is only 2.4% lower than the experimental value reported.

Conclusion

We simulate the dissociation of MH by depressurization in a sandstone core with a simple one-dimensional model. We integrate the governing equations in time by a fifth order accurate scheme, and we discretize the equation in space with the finite difference method and polynomial interpolation curves, retaining a second order accuracy. By comparing our numerical predictions with experimental results of (Masuda et al., 1999), we find a good concordance for the amount of gas produced. Additionally, we do not observe any strong pressure and temperature delay among different sections of the core. Our numerical scheme is easier to implement compared to implicit methods, but it poses severe limitations on the step size used.

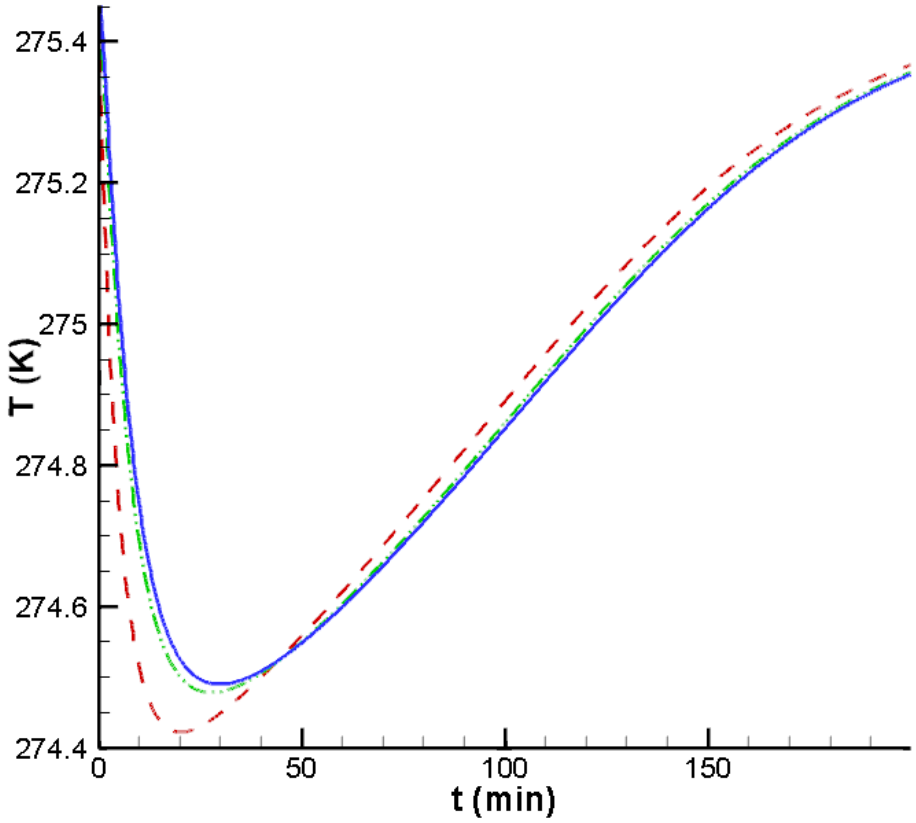

Figure 2 Temperature change with time at three different sections of the sandstone core. Red dashed line at x=0.75 cm, green dashed dot dot line at x=15 cm, and blue solid line at x=22.5 cm.

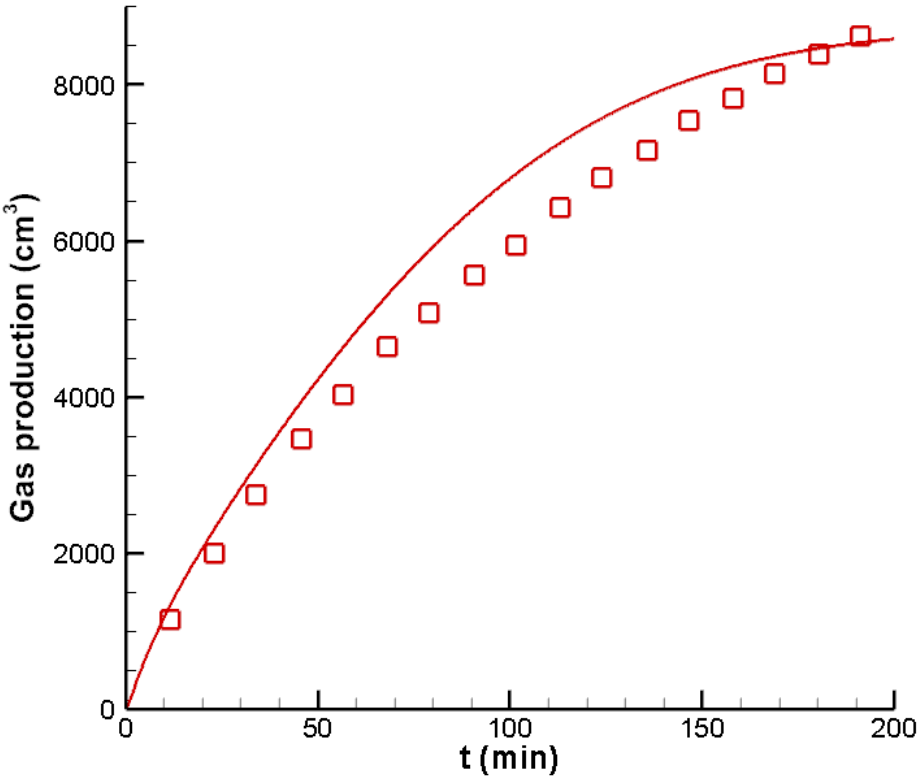

Figure 3 Cumulative amount of methane gas produced with time during the dissociation process. Red solid curve numerical results, red open squares experimental values of (Masuda et al., 1999)

Literature

Sloan, D., Koh, C., 2007: "Clathrate Hydrates of Natural Gases, Third Edition", September 7, CRC Press, pp. 752, ISBN 9780849390784

Kvendvolden, K., 1993: "Gas Hydrates - Geological Perspective and Global Change", Rev Geophys. Vol. 31, No 2, pp.173-187

Sun, X., Nanchary, N., Mohanty, K.K., 2005: "1-D modeling of hydrate depressurization in porous media", Transport in Porous Media, Vo. 58, No. 3, pp. 315–338

Zhao J., Ye C., Song Y., Liu W., Cheng C., Liu Y., Zhang Y., Wang D., Ruan X., 2012: "Numerical Simulation and Analysis of Water Phase Effect on Methane Hydrate Dissociation by Depressurization", I & EC research, Vol. 51, pp. 3108-3118

Ruan X., Song Y., Zhao J., Liang H., Yang M., Li Y., 2012: "Numerical Simulation of Methane Production from Hydrates induced by Different Depressurizing Approaches ", Energies, Vol. 5, No. 2, pp. 438–458

Nazridoust, K., Ahmadi, G., 2007: "Computational modeling of methane hydrate dissociation in a sandstone core", Chemical Engineering Science, Vol. 62, No. 22, pp. 6155–6177

Sun, X. & Mohanty, K.K., 2006: "Kinetic simulation of methane hydrate formation and dissociation in porous media", Chemical Engineering Science, Vol. 61, No. 11, pp. 3476–3495

Masuda, J., Fujinaga, Y., Naganawa, S., Fujita, K., Sato, K., Hayashi, Y., 1999: "Modeling and experimental studies on dissociation of methane gas hydrates in Berea sandstone cores", Proceedings of Third International Conference on Gas Hydrates. Salt Lake City, Utah, USA.